ÎMBUNĂTĂȚIREA CARACTERISTICILOR FIZICO-MECANICE ȘI STRUCTURALE A ALIAJELOR Mg-Zn-(Mn) OBȚINUTE PRIN TEHNICA SPS

IMPROVING THE PHYSICAL-MECHANICAL AND STRUCTURAL CHARACTERISTICS OF Mg-Zn-(Mn) ALLOYS OBTAINED BY SPS TECHNIQUE

VIOLETA TSAKIRIS, DORINEL TĂLPEANU* , MAGDALENA VALENTINA LUNGU, DELIA PĂTROI, GABRIELA BEATRICE SBÂRCEA, VIRGIL EMANUEL MARINESCU

National Institute for Research and Development in Electrical Engineering ICPE-CA, Splaiul Unirii 313, Bucharest, Romania

For the replacement and regeneration of hard and damaged tissues, it is preferable to use orthopedic implants from Mg-based biomaterials. It is desirable that orthopedic implants have mechanical properties similar to those of natural bone to avoid the effect of stresses due to the difference in properties of materials, i.e. between bone and implant. Numerous studies have shown that of all metallic biomaterials, Mg used as an orthopedic biomaterial can promote bone reconstruction and accelerate the healing process, having both density and modulus of elasticity close to cortical bone.

In this paper, Mg-Zn-(Mn) biomaterials with 5 wt.% Zn and/without a small addition of Mn (0.3 wt.%) were synthesized by high-energy mechanical milling of the component powders mixtures and consolidated by Spark Plasma Sintering technique, at different sintering temperatures (350, 400 and 450°C) to be used as orthopedic implants. The influence of the mechanical milling and sintering parameters, on the chemical, structural and physical characteristics was investigated. Properties suitable for the intended application, in terms of physical properties such as density 1.77-1.78 g/cm^3, hardness (95-112 HV), and Young Modulus (36-46 GPa) recommend the alloys obtained from Mg-Zn-(Mn), as potential biomaterials. These biomaterials resulted from the composite powder mechanical milled for 5 h and sintered at the highest sintering temperature (450°C).

Pentru înlocuirea și regenerarea țesuturilor dure și deteriorate, se preferă utilizarea implanturilor ortopedice din biomateriale pe bază de Mg. Este de dorit ca implanturile ortopedice să aibă proprietăți mecanice similare cu cele ale osului natural pentru a evita efectul tensiunilor datorat diferenței de proprietăți dintre materiale, adică dintre os și implant. Numeroase studii au arătat că, dintre toate biomaterialele metalice, Mg folosit ca biomaterial ortopedic poate favoriza reconstrucția osoasă și poate accelera procesul de vindecare, având atât densitatea cât și modulul de elasticitate apropiate de al osului cortical.

În această lucrare, biomaterialele Mg-Zn-(Mn) cu 5%gr. Zn, cu/fără un adaos mic de Mn (0.3 %gr.), au fost sintetizate prin măcinarea mecanică de înaltă energie a amestecurilor de pulberi componente și consolidate prin tehnica Spark Plasma Sintering, la diferite temperaturi de sinterizare (350, 400 și 450°C), pentru a fi utilizate ca implanturi ortopedice. S-a investigat influența parametrilor mecanici de măcinare și sinterizare asupra caracteristicilor chimice, structurale și fizice. Proprietăți adecvate pentru aplicația vizată, în ceea ce privește proprietățile fizice, cum ar fi densitatea 1.77-1.78 g/cm^3, duritatea (95-112 HV) și modulul Young (36-46 GPa) recomandă aliajele Mg-Zn-(Mn) obținute, ca potențiale biomateriale. Aceste biomateriale au rezultat din pulberea compozită măcinată mecanic timp de 5 ore și sinterizată la cea mai mare temperatură de sinterizare (450°C).

Keywords: doped magnesium, biomaterial, SPS technique, osseous implants

1.Introduction

Recent orthopedic surgery is largely dependent on the development of biomaterials used to repair fractures and replace joints. Biomaterials make a significant contribution to improving health and the well-being of the quality of human life. Mg is a reactive metal being prone to higher corrosion rates compared to other metals and therefore it is advisable to consider its corrosion behavior when designing and developing an Mg alloy with certain properties for a specific application. Applications like biodegradable orthopedic implants require certain material characteristics such as, mechanical properties close to natural bone, biocompatibility, and degradation in a corrosive environment at a rate slow enough to allow healing. Biodegradable implants dissolve in the human body and are eliminated after the convalescence period of the fractured bone, so the implant removal operation is no longer necessary [1, 2].

Of all the metals, Mg has stood out because it has mechanical properties close to the bone and corrodes at pH levels ranging from 7.4 to 7.6 as in the case of an advanced corrosion environment, as found in physiological systems. The only problem that arises in clinical applications is its high rate of degradation. Therefore, researchers are making great efforts to develop alloys that are compatible with implant applications but also ensure a degradation rate in tandem with the healing process, thus with improved corrosion resistance. Elements such as Ca, Zn, Mn, and rare earth elements are used for alloying of Mg to ensure the above

* Autor corespondent/*Corresponding author*,
E-mail: dorinel.talpeanu@icpe-ca.ro

requirements [2]. It was found that Ca has an added benefit in bone growth and some rare earth elements, such as Ce and Y, have toxic effects on cells although it contributes to the reduction of the Mg corrosion rate [2]. Some researchers have shown that by using an antimicrobial metal such as copper, the antibacterial capacity of an Mg alloy can be increased [3, 4].

Zn and Mn although ensure good compatibility, the added amount must be modulated to achieve an optimum of mechanical properties and of resistance to corrosion.

Zinc is one of the biodegradable and non-toxic elements, which involves the synthesis of various enzymes in the human body and has anti-inflammatory actions, as shown in the works [5–7]. On the other hand, Zn and Mg have the same hexagonal closed crystal structure (HCP) [8]. Recently it has been shown that Mg-Zn alloy has potential for implant applications. However, in most research, in Mg-Zn alloys manufactured by traditional powder metallurgy (PM) or by casting, there are also residual phases such as $MgZn_2$, Mg_2Zn_{11} etc. [9-11]. These secondary phases can play an important role in increasing the mechanical properties but their influence on the corrosion behaviour is stronger because they act as cathodes in relation to the magnesium matrix and causes galvanic corrosion, which leads to localized corrosion in degradation. Therefore, even if the mechanical properties corresponding to the implantation are ensured, the content of the phases $MgZn_2$, Mg_2Zn_{11} must be reduced [8].

Compared to traditional PM or casting, the sintering processes by SPS (Spark Plasma Sintering) have not only the ability to rapidly densify and control the growth of granulation, but also has a sufficient metallurgical reaction [12] for consolidation. This method appears to be the most efficient and convenient method for a wide variety of metals, alloys, and composites [13–15].

The mechanical and corrosion performance of biomaterials for implants depends on the microstructure of the alloy, the selected chemical composition, the manufacturing process, the heat treatment, and the alloying elements that vary depending on the type and quantity of the elements [16-23]. Regarding the mechanical properties, for orthopaedic implants, it is necessary to be close to the bone values [24], namely:

- *natural bone*: density: 1.8-2.1 g/cm^3; Young Modulus: 3-20 GPa; compressive strength: 110 MPa
- *biodegradable Mg alloy*: density: 1.74-2.0 g/cm^3; Young Modulus: 41-45 GPa, compressive strength: 200 MPa.

Orthopedic applications should provide mechanical integrity that protects the bone for up to 12-18 weeks before the bone tissue heals [25] and the corrosion rate should be less than 0.5 mm/year in the simulated body fluid of 37 ° C (SBF) [26].

In the present work, biocompatible materials such as Zn and/without Mn have been mechanical milled with magnesium (Mg) and then plasma sintered to develop novel biomaterials with improved mechanical properties.

The aim of this research was to study the effect of mechanical milling (MM) and SPS technical parameters to find the optimal processing parameters to obtain improved physico-chemical, structural and mechanical properties so that these materials can be used for orthopedic implants.

2. Experimental procedure

The raw powder materials in powder form, such as Mg, Zn, and Mn, were provided by the Alfa Aesar, Germany, as follows:

- Pure Mg powder of min. 99.8%;
- Pure Zn powder of min. 99.9%;
- Pure Mn powder of min. 99.95%.

The petroleum ether with a boiling range of 40-60°C was used as a milling agent and was supplied from SC Chimreactiv SRL, Romania.

Given the high degree of reactivity of the experimental powders, both unsealing and handling/weighting for dosing to the desired compositions were performed inside a Glovebox, in a controlled atmosphere (Ar).

The chemical compositions of the powders mixtures from the Mg-Zn-(Mn) system are presented in Table 1.

Table 1
Chemical compositions of the powders mixtures from the Mg-Zn-(Mn) system/
Compoziția chimică a amestecurilor de pulberi din sistemul Mg-Zn-(Mn)

Material	Specimen code	Chemical composition (wt.%)		
		Mg	Zn	Mn
Mg-Zn	AM1	95	5	-
Mg-Zn-Mn	AM2	94.7	5	0.3

The mixtures of AM1 and AM2 composite powders were made in batches of 50 g each, by mechanical homogenization of the initial powders, dosed according to the recipes established in Table 1, in a planetary ball mill of Retsch PM 400 type. Prior to the milling process of the powder mixtures, the milling bowls, and the milling medium (stainless steel balls) were cleaned by washing with petroleum ether for 1 hour in the mill and then, washed by hand with acetone. The loading of the powder mixtures dosed for MM and the milling media in the bowls, as well as the addition of petroleum ether were carried out in a glovebox, in Ar atmosphere.

For the MM process, stainless steel bowls with a capacity of 500 ml were used and as milling media, stainless steel balls of different diameters (5, 10, 12, 14, 15 and 19 mm) have been used, in a total quantity of 50 g

Table 2

Composite materials and MM processing parameters of the experimental powder mixtures
Materiale compozite şi parametrii de procesare prin MM a amestecurilor de pulberi experimentale

Composite powder materials/weight	**MM conditions**
Mg-Zn (ME1-AM1) 47.5-2.5 (g) Mg-Zn-Mn (ME2-AM2) (47.35-2.5-0.15) (g)	• B/P: 10:1 • V_{rot}: 300 rpm • Stainless steel bowls of 500 ml • Milling medium: stainless steel balls of various diameters • Milling agent: petroleum ether • Effective milling time: 5 h. • Milling atmosphere: Ar.

The milling process took place in Ar atmosphere, with 5 minutes break after every 15 minutes of MM, both clockwise and counter clockwise, the total milling time being 6 hours and 35 minutes.

The types of composite powder mixtures made from the two systems Mg-Zn (ME1-AM1) and Mg-Zn-Mn (ME2-AM2), and the processing parameters by MM in protective atmosphere of Ar and in humid environment (petroleum ether) are presented in Table 2.

After milling, the mixtures of the obtained composite powders were stored in petroleum ether and kept in a glovebox under Ar atmosphere, until the investigation of their structural, physical, chemical properties and their processing by SPS.

Consolidation of composite powders was performed in vacuum with a SPS installation, HP D25 type (FCT System GmbH, Germany). The sintering temperature of the composite powders was 350°C, 400°C and 450°C. The holding time on the sintering temperature was 5 minutes and the pressing pressure varied between 2.5 - 40 MPa. The pulse scheme for SPS consolidation of the Mg-based alloys is shown in Fig. 1 [27] and the technological flux is presented in Fig. 2.

The qualitative phase determination by X-ray diffraction of the initial Mg, Zn, and Mn powders, as well as of the Mg-Zn and Mg-Zn-Mn composite materials obtained by MM was performed using the diffractometer D8Discover, Bruker-Germany, configured on primary optics with a tube with primary Cu radiation (λ = 1.540598Å), Göebel mirror and on secondary optics with a 1D LynxEye detector. Diffractograms were recorded in an angular increment of 0.040, at a scan rate of 0.5s / step, in the measuring range of 2θ = 10°-100°. The qualitative analysis was performed using the ICDD Release 2014 database.

Considering the main crystallographic phases, the Rietveld analysis determined the parameters of the elementary cell, respectively the average crystallite size.

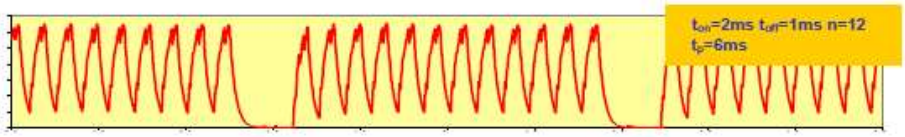

Fig.1 - Pulse scheme used for SPS consolidation of Mg alloys/
Schema de impulsuri utilizată pentru consolidarea SPS a aliajelor Mg

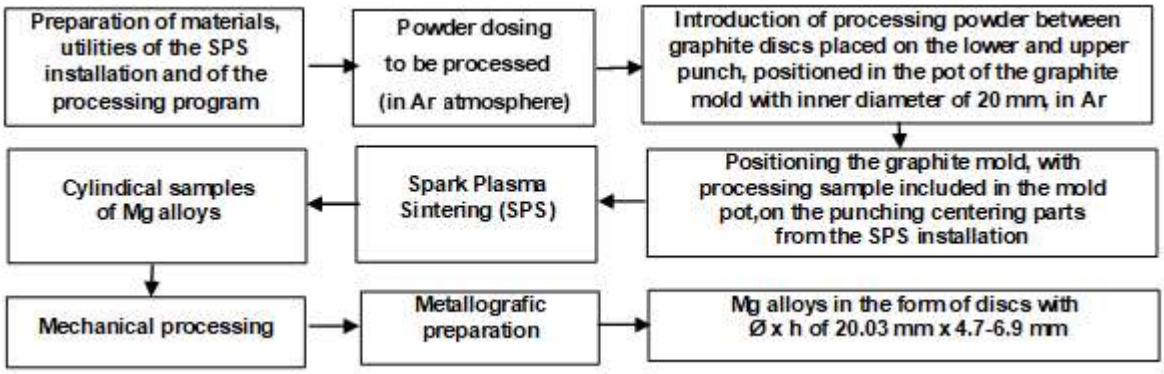

Fig.2 - The technological flux of Mg-Zn-(Mn) alloys through the SPS process/
Fluxul tehnologic al aliajelor Mg-Zn-(Mn) prin procesul SPS

The scanning electron microscopy / energy-dispersive X-ray (SEM / EDX) analysis of the initial Mg, Zn, and Mn powders, as well as of the Mg-based composite powders (Mg-Zn and Mg-Zn-Mn) were performed with a scanning electron microscope with field emission source and with ion focused beam (FESEM-FIB) type Auriga Zeiss. This instrument is equipped with an EDS SDD probe, X-MaxN, Oxford Instruments, at x 500 magnification and at an acceleration voltage of 10 kV.

Optical Microscopy (OM), SEM and EDX were performed on metallographically prepared sintered samples (by using SiC grit 800, 1000, 1200, 2000, 4000 metallographic papers, in an aqueous medium, and polishing with 3 µm diamond suspension - Struers) until a mirror surface was obtained, on sintered samples of diameter 20.02-20.03 mm and height of 4.7-6.9 mm. No chemical attack was used for the surfaces of the samples to be analysed.

The MO analysis of the sintered samples was carried out with an inverted metallographic microscope Kern OLM 171, at x 1000 magnification.

Determination of indented hardness (H_{IT}), Vickers hardness HV, Young Modulus (E_{IT}), elastic contact stiffness (S), mechanical deformation elastic work ($W_{elastic}$), mechanical deformation plastic work ($W_{plastic}$) and elasticity index (η_{IT}) were performed by nanoindentation tests, in accordance with the standards ISO 14577-1: 2015 and ISO 14577-4: 2016.

The tests were realized at room temperature on a Micro-Combi Tester equipment (CSM Instruments, Switzerland), equipped with nanoindentation mode (NHT) with a Berkovich diamond indenter, at the following working parameters:

- Maximum indentation force, P_{max}: 300 ± 1 N;
- Approach speed of the test indenter: 2000 nm/min;
- Linear loading speed / unloading speed: 600 N/min;
- Data acquisition frequency: 10 Hz;
- Poisson's ratio of Mg alloy sample (ν = 0.29).

Ten measurements were done on each sample, the average values being presented.

The calculation method used in determining the values of mechanical properties was the Oliver & Pharr method.

3. Results and discussions

All powder particles had irregular shapes (depending on the obtaining process) and various micron sizes.

In Fig. 3 (a-c), the morphological aspects of the initial Mg, Zn, and Mn powders are shown.

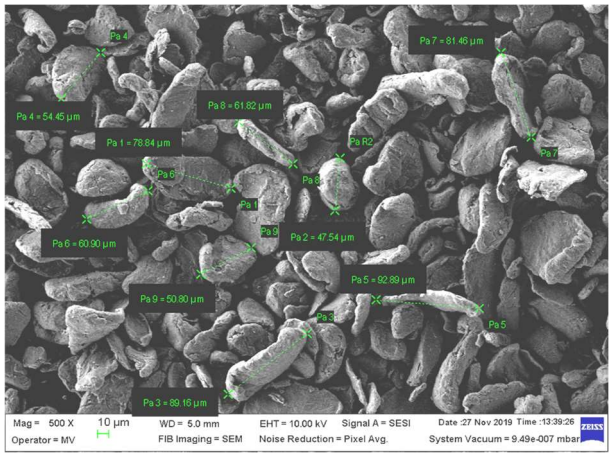

a

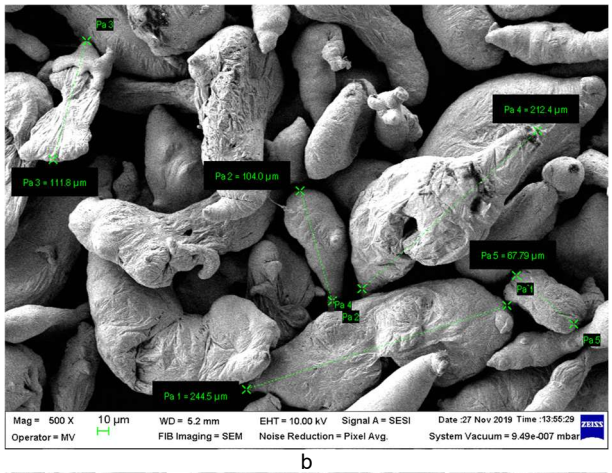

b

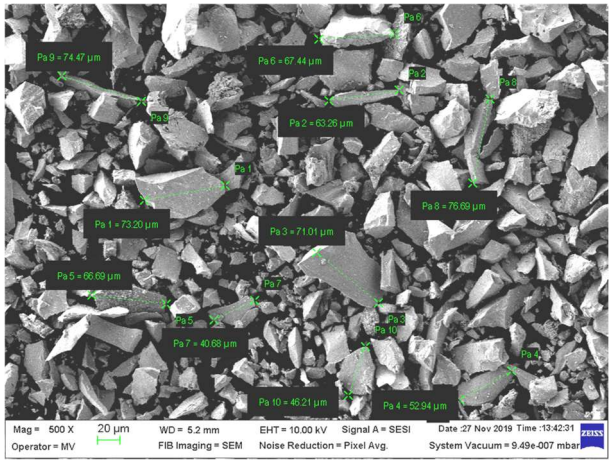

c

Fig.3 - SEM images of initial Mg (a), Zn (a) and Mn(c) powders, x 500/ *Imagini SEM pentru pulberile inițiale de Mg (a), Zn (a) și Mn (c), x 500*

Mg has particles with irregular, oval shapes, and mostly uniform dimensions, ranging from 47 to 92 µm, and the average particle size was approx. 69 µm (Fig. 3 a).

Zn particles have accentuated irregularities and longer shapes. From a dimensional point of view, Zn particles have a varied dimensional range, for example from 67 µm to 2445 µm, an average particle size being approx. 775 µm (Fig. 3 b).

Mn particles have an irregular shape, with an angular appearance and a varied dimensional

range (40 - 76 μm), having a particle average size of approx. 60 μm (Fig. 3 c).

The XRD analysis revealed the crystalline nature of the initial Mg, Zn, and Mn powders, as well as the Mg-Zn and Mg-Zn-Mn composite powders.

For the Mg powder, the diffraction peaks correspond to the hexagonal crystalline structure of Mg having the network parameters a = 3.206 Å and c = 5.206 Å, according to the ICDD sheet PDF Nr. 01-089-4244.

For the Zn powder, the diffraction peaks correspond to the hexagonal crystalline structure, with the network parameters a = 2.661 Å and c = 4.945 Å, according to the ICDD sheet PDF Nr. 01-087-0713.

For the Mn powder, the diffraction peaks correspond to the cubic crystalline structure, having the lattice parameter a = b = c = 8.900 Å, according to the ICDD sheet PDF Nr. 00-020-0180.

In the case of Mg-Zn and Mg-Zn-Mn composite powders, the diffraction lines corresponding to the crystalline phases of Mg and Zn were highlighted, as expected. Zinc being in a too-small proportion (only 5%), the most pronounced peak for this element was obtained at 2θ = 43°, for both composite powders.

By MM the mixtures of Mg-Zn-(Mn) powders for 5 hours, in Ar atmosphere and petroleum ether, a finishing effect is obtained on the crystallite size of the Mg and Zn phases as the Rietveld quantitative analysis confirmed. Therefore, the crystallite size of the component phases from the mechanically alloyed composite powders ME1-AM1 and ME2-AM2, decreased for Mg by about 1.5-1.6 times and for Zn, decreased by about 1.6-1.8 times. The too low concentration (0.3 wt. %) of Mn in ME2-AM2, could not be evaluated by X-ray analysis, this element being below the detection limit of the apparatus.

EDX elemental analysis on selected areas of composite particles has shown the existence of spectral lines corresponding to the constitutive and predominant phases of the resulting composite powders: Mg (93.9-94 wt.%) and Zn (1.7-2.3 wt.%). Mn could not be evaluated in percentage by weight, in the analysed areas being in a too low content (0.3 %).

In the Fig. 4 (a, b), the XRD analysis revealed the existence of both crystalline phases (Mg and Zn), after the sintering process of Mg-5%Zn and Mg-5%Zn-0.3%Mn at 450°C/5 min.

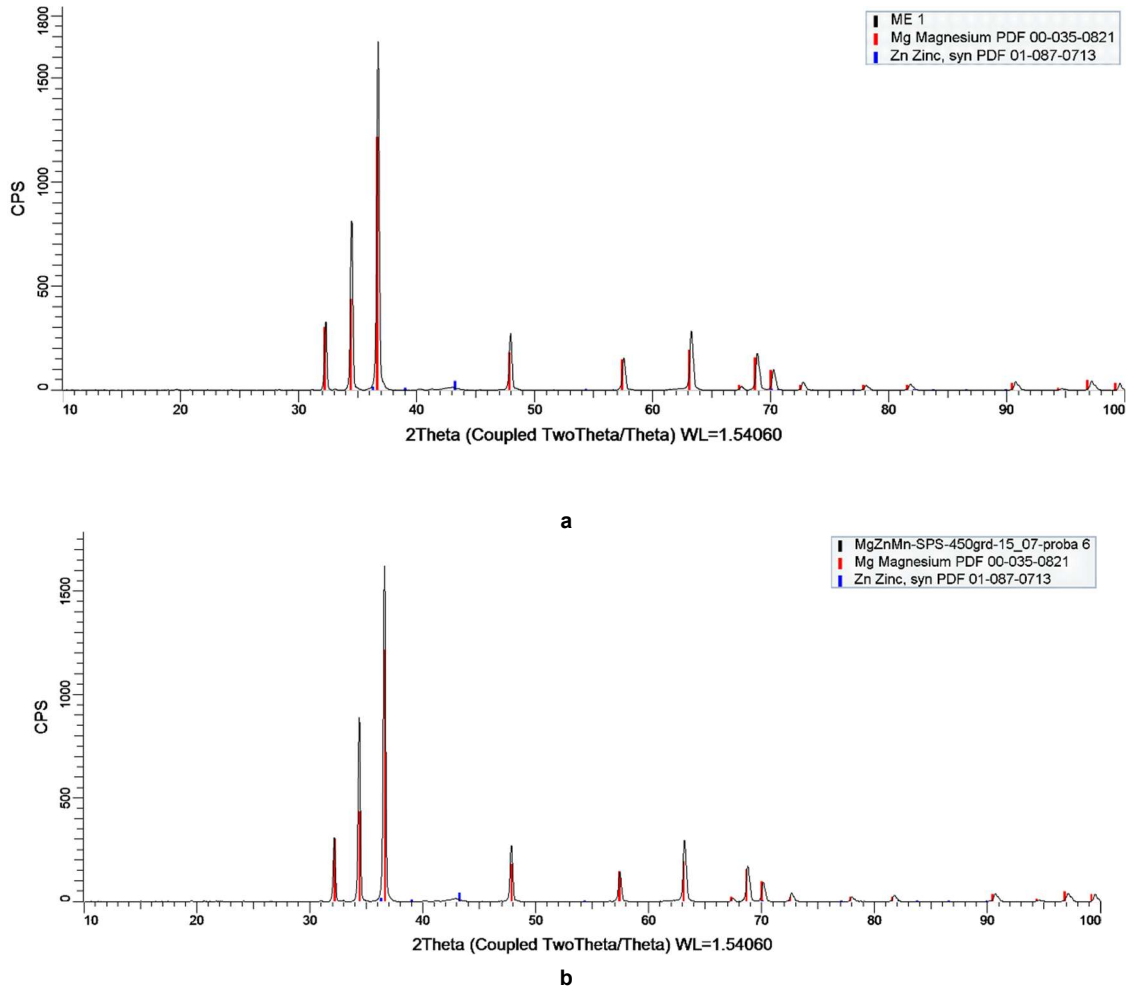

Fig. 4 - XRD Difractograms of the Mg alloys procesed by SPS at 450 °C: (a) ME3-S Mg-5%Zn (b) ME6-S Mg-5%Zn-0.5%Mn/ *Difractogramele XRD pentru aliajele de Mg procesate prin SPS la 450°C: (a) ME3-S Mg-5%Zn (b) ME6-S Mg-5%Zn-0.3%Mn*

Table 3

Density of samples sintered by SPS from composite powders Mg-based/
Densitatea probelor din pulberi compozite pe bază de Mg sinterizate prin SPS

Experimental Models	Material	$T_{sintering}$ (°C)/min	Volumetric Density (ρ_{sint}), g/cm^3	Theoretical density (ρ_{th}), g/cm^3	Total porosity (P_t), %	Degree of compactness (ρ_{rel}), %
ME1-S	Mg-5%Zn	350/5	1.1774	1.8063	34.82	65.18
ME2-S	Mg-5%Zn	400/5	1.2039	1.8063	33.35	66.65
ME3-S	Mg-5%Zn	450/5	1.7710	1.8063	1.96	98.04
ME4-S	Mg-5%Zn-0.3%Mn	350/5	1.2013	1.8106	33.65	66.35
ME5-S	Mg-5%Zn-0.3%Mn	400/5	1.2079	1.8106	33.29	66.71
ME6-S	Mg-5%Zn-0.3%Mn	450/5	1.7819	1.8106	1.58	98.42

The density of Mg-based alloys elaborated by the SPS technique was determined by the volumetric method, obtaining the lowest degree of compactness (approx. 66%) for the sintered samples at 350 and 400°C.

Table 3 presents the values of volumetric density, the total porosity, and the degree of compactness, related to the values of theoretical density.

The theoretical densities (ρ_{th}) of the mixtures of composite powders AM1 (Mg-Zn) and AM2 (Mg-Zn-Mn) from Table 1, were calculated with the mixture rule, considering the theoretical densities of Mg, Zn and Mg, respectively: 1.738 g/cm^3, 7.14 g / cm^3 and 7.21 g / cm^3, respectively.

The relative density (ρ_{rel}) or degree of compactness of the sintered samples was determined with relation 1 and the total porosity (P_t) of the sintered samples was determined with relation 2 [28]:

$$\boldsymbol{\rho_{rel} = 100 * \frac{\rho_{sint}}{\rho_{th}} = Pt - 100}\ [\%] \qquad (1)$$

$$\boldsymbol{P_t = 100 * \left(1 - \frac{\rho_{sint}}{\rho_{th}}\right)}\ [\%] \qquad (2)$$

From the analysis of the density values of the sintered samples, it is found that the highest degree of compactness (98.4% and 98.42%, respectively), was obtained for the ME3-S and ME6-S samples, sintered at the highest temperature (450°C), the other samples having a low degree of compactness (33-34%).

The OM images of the Mg-based alloys (ME3-S, Fig. 5a) and (ME6-S, Fig. 5b) obtained by SPS have shown microstructures with a high degree of homogeneity.

According to the Mg-Zn binary diagram, the solubility of Zn in the Mg matrix is about 6 wt.% at 480°C. When the SPS sintering temperature reaches the melting point of Zn (420°C), by means of discharging sparks and pressure as well as by heating, through the Joule effect, between the powder particles and Zn particles transformed into a liquid, the diffusion of Zn into Mg is accelerated. In fact, this method is equivalent to a solid-liquid phase sintering method [5].

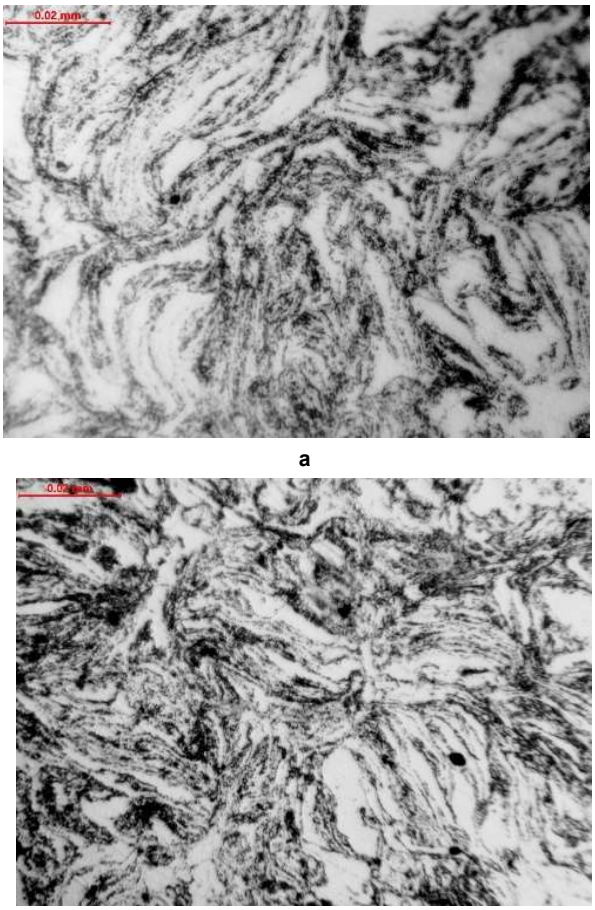

a

b

Fig. 5- OM images of samples from Mg alloys:(a) ME 3-S, (b) ME6-S, x 1000/ *Imagini prin microscopie optică (MO) ale probelor din aliaje de Mg:(a) ME 3-S, (b) ME6-S, x 1000*

In Fig. 6, the SEM images, and the results of the EDX elemental analysis of the Mg alloy ME3-S elaborated by SPS at 450°C /5 min, in vacuum at P = 40 MPa are presented.

SEM images and EDX elemental analysis (Fig. 6) show that the Mg-Zn alloy has homogeneous microstructures, with a uniform dispersion of Mg and Zn elements, as well as the existence of nanometric areas of molten Zn (100-200 nm) in the base matrix, with uniform distribution, for the Mg alloy (ME3-S).

Due to both metallographic preparation and analysis system some oxygen content (6.5 wt. %) has been detected.

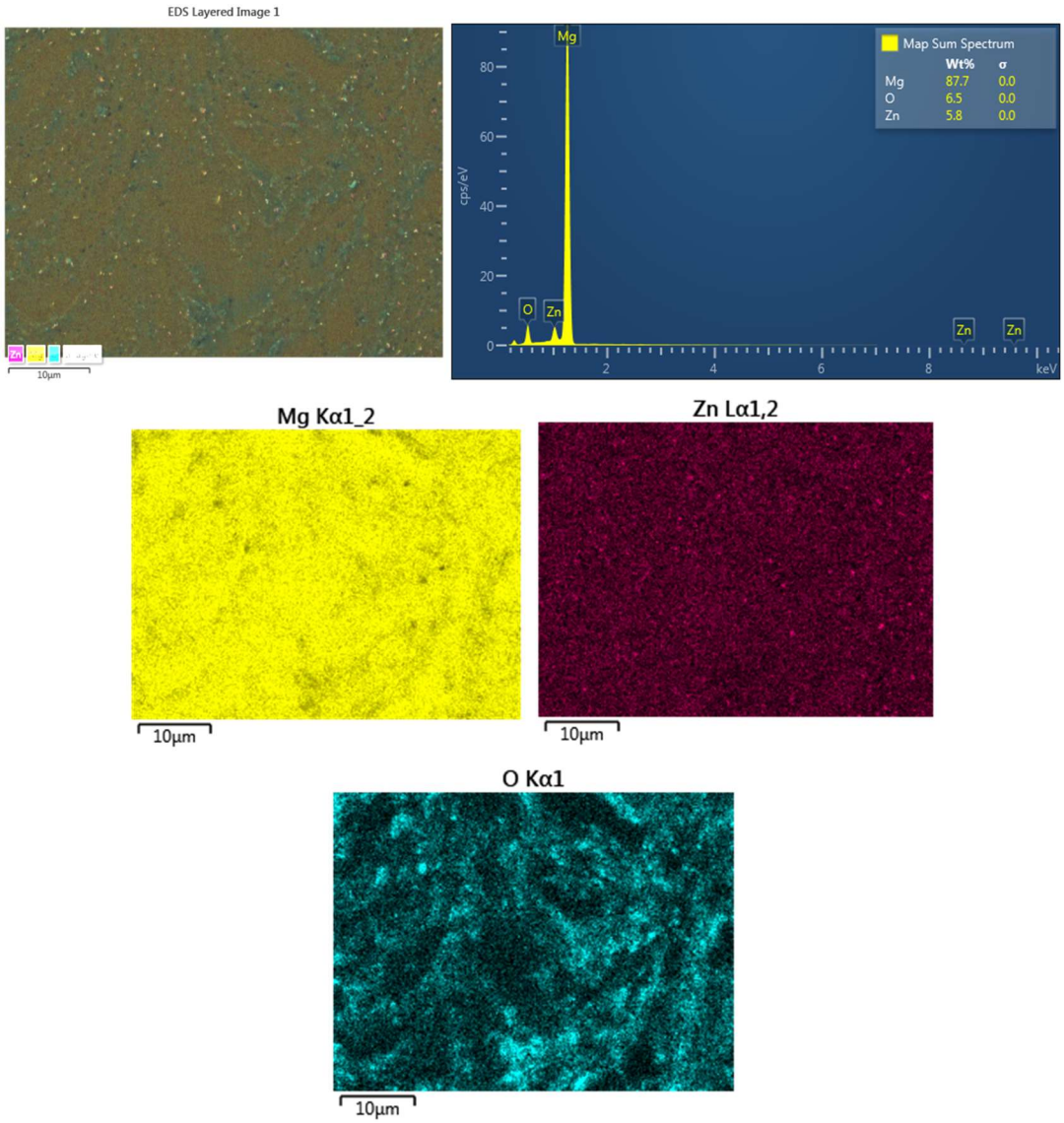

Fig. 6 - EDX results of the sintered plasma magnesium alloys ME3-S/ *Rezultate EDX ale aliajelor sinterizate în plasmă ME3-S*

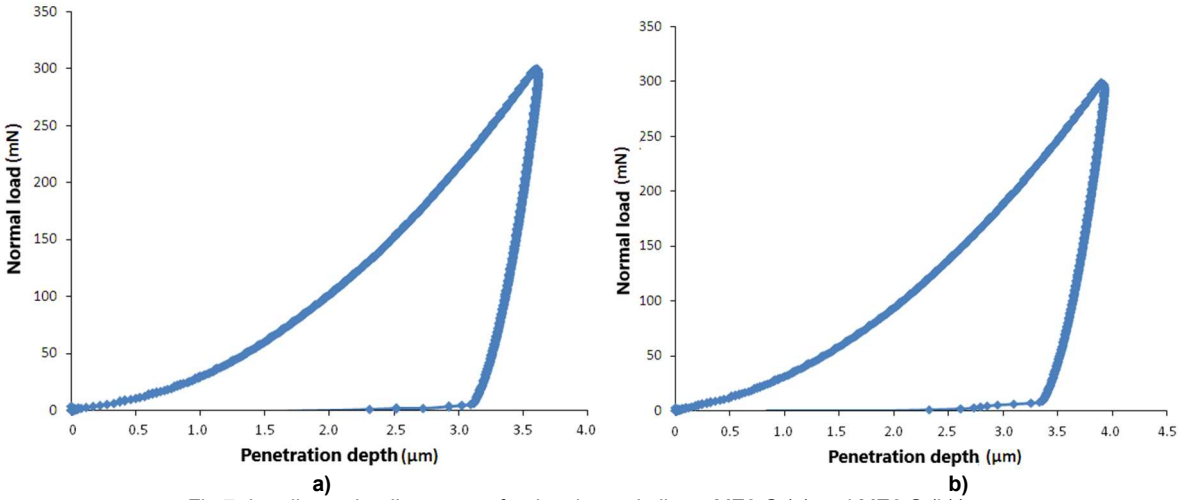

Fig.7 -Loading-unloading curves for the sintered alloys: ME3-S (a) and ME6-S (b)/
Curbe de încărcare-descărcare pentru aliajele sinterizate: ME3-S (a) and ME6-S (b)

Table 4

Values of hardness (H_{IT}, HV), Young Modulus (E_{IT}), maximum indentation penetration depth (h_{max}) and elastic contact stiffness (S) for the sintered samples/*Valorile durității (H_{IT}, HV),ale modulului Young (E_{IT}), adâncimii de penetrare maximă prin identare (h_{max}) și rigiditatea de contact elastic (S) pentru probele sinterizate*

Experimental Models	H_{IT} (GPa)	HV	E_{IT} (GPa)	h_{max} (nm)	S (mN/nm)
ME1-S	**0.089 ± 0.036**	**8 ± 3**	**9 ± 2**	**12744 ± 2564**	**0.68 ± 0.014**
ME2-S	**0.130 ± 0.028**	**12 ± 3**	**6 ± 2**	**10697 ± 1028**	**0.383 ± 0.088**
ME3-S	**1.03 ± 0.068**	**95 ± 6**	**36 ± 2**	**3915 ± 120**	**0.767 ± 0.025**
ME4-S	**0.204 ± 0.030**	**19 ± 3**	**11 ± 2**	**8460 ± 598**	**0.533 ± 0.079**
ME5-S	**0.248 ± 0.069**	**23 ± 6**	**10 ± 1.5**	**7913 ± 955**	**0.436 ± 0.008**
ME6-S	**1.22 ± 0.117**	**112 ± 11**	**46 ± 2**	**3604 ± 158**	**0.877 ± 0.012**

Table 5

Values of the mechanical work of elastic deformation ($W_{elastic}$), of the mechanical work of plastic deformation ($W_{plastic}$), of the index of elasticity (η_{IT}) and of the index of plasticity (100 - η_{IT})/ *Valorile lucrului mecanic de deformare elastică ($W_{elastic}$), indicelui de elasticitate (η_{IT}) și indicelui de plasticitate (100 - η_{IT}).*

Experimental Models	W_{elast} (nJ)	W_{plast} (nJ)	W_{total} (nJ)	η_{IT} (%)	100 - η_{IT} (%)
ME1-S	58.594 ±12.718	1254.59 ±428.76	1311.18 ±416.05	4.868 ±2.515	95.132 ±2.515
ME2-S	31.558 ±19.591	1476.192 ±227.087	1507.71 ±217.95	2.197 ±1.658	97.803 ±1.658
ME3-S	61.364 ±2,973	370.46 ±18.887	431.824 ±17.956	14.237 ±1.002	85.763 ±1.002
ME4-S	67.944 ±31.644	706.503 ±396.37	774.45 ±365.85	11.392 ±8.969	88.608 ±8.969
ME5-S	56.57 ±43.48	1055.78 ±324.40	1112.35 ±283,15	5.857 ±4.664	94.143 ±4.664
ME6-S	53.607 ±1.161	328.28 ±12.93	381.887 ±13.371	14.048 ±0.452	85.952 ±0.452

In addition, the analysis of SEM and EDX for the ME6-S samples has revealed similar aspects in terms of structural characteristics and chemical composition.

In Fig. 7 (a, b), the loading-unloading curves for the sintered alloys ME3-S and ME6-S are presented.

Tables 4 and 5 present the mechanical properties resulting from the nanoindentation tests on the samples sintered at 450°C for 5 min, obtained by using the SPS technique, in vacuum and under 40 MPa pressure.

The value of the elastic deformation is given by the area described by the discharge curve and perpendicularly drawn from the maximum indentation force to the OX axis. All Mg alloys showed both plastic deformation and an elastic deformation when applying the indentation force during the loading/unloading cycle, according to the graphs and the tables above. It is known that the elastic contact stiffness is given by the tangent to the discharge curve and is defined as the ratio between the indentation force (F_n) and the penetration depth (d_h).

From the point of view of the elastic contact stiffness, the materials support an important plastic deformation (area delimited by the loading curve and the unloading curve), also confirmed by the values obtained for the plasticity index (100 - η_{IT}).

Mg alloys show variations in mechanical properties, depending on the sintering temperature and composition. Mg-5% Zn alloys have lower hardness and Young modulus values compared to those obtained for Mg-5% Zn-0.3% Mn alloys, Mn having an important influence in the finishing of the granulation and implicitly, in the hardening of the matrix. Also, it is found that the hardness values increased with the increase of the sintering temperature, and regarding the values of the Young Modulus, the highest values are obtained at the highest sintering temperature (450°C). It is noted that the Mg-5% Zn-0.3% Mn alloy, processed by SPS at 450°C, for 5 min, has the best mechanical properties, compared to other samples of Mg alloy processed at lower temperatures.

4. Conclusions

As shown by the results of elemental analysis by XRF, SEM, and EDX, two dense (max 2% porosity) and homogeneous Mg-Zn-(Mn) alloys were obtained by SPS at a sintering temperature of 450°C with a holding time of 5 minutes.

Investigations performed by X-ray diffraction, optical microscopy, electron microscopy, and chemical mapping revealed the presence of crystalline phases of Mg and Zn and Mn, both in the composite powder mixtures and in the sintered ones. No secondary phases were detected.

The Mg-based alloys obtained by SPS in vacuum, at a sintering temperature of 450°C/5 min and at the maximum pressure of 40MPa, have appropriate physical (density of 1.77 ... 1.78 g/cm^3) and mechanical (Vickers hardness 95 .. 112 HV and Young Modulus 36 .. 46 GPa) properties.

For both studied alloys, much better values of density and mechanical properties were obtained than those reported for degradable Mg alloys, i.e. closer to those needed for human bone, which is why it is considered that both alloys have the potential to be used as orthopedic implants.

Further studies related to the corrosion behaviour of the studied Mg-Zn-(Mn) alloys are envisaged to establish their degradation parameters.

ACKNOWLEDGMENTS

This work was supported by the Romanian Ministry of Research, Innovation and Digitalization, project number 25PFE/30.12.2021 – Increasing R-D-I capacity for electrical engineering-specific materials and equipment with reference to electromobility and "green" technologies within PNCDI III, Programme 1 and project no. PN19310102/2019 under the contract no. 46N/2019.

REFERENCES

[1] SV S. Prasad, SB Prasad, K. Verma, R. K. Mishra, V. Kumar, S. Singh, The role and significance of Magnesium in modern day research-A review, Journal of Magnesium and Alloys, 2022, **10** (1), 1.

[2] V.Tsakiris, C.Tardei, F. M. Clicinschi, Biodegradable Mg alloys for orthopedic implants – A review, Journal of Magnesium and Alloys, 2021, **9** (6), 1884.

[3] D. Chen, Y. He, H. Tao, Y. Zhang, Y. Jiang, X. Zhang, S. Zhang, Biocompatibility of magnesium-zinc alloy in biodegradable orthopedic implants, International Journal of Molecular Medicine, 2011**, 28** (3), 343.

[4] W. Zhang, M.-C. Zhao, Z. Wang et al., Enhanced initial biodegradation resistance of the biomedical Mg-Cu alloy by surface nanomodification, Journal of Magnesium and Alloys, https://doi.org/10.1016/j.jma.2021.12.013 (in press)

[5] C. Xiao, L. Wang, Y. Ren, S. Sun, E. Zhang, C. Yan, Q. Liu, X. Sun, F. Shou, J. Duan, H. Wang, G. Qin, Indirectly extruded biodegradable Zn-0.05wt%Mg alloy with improved strength and ductility: In vitro and in vivo studies, Journal of Materials Science & Technology, 2018, **28** (9) 1618.

[6] Z. Tang, J. Niu, H. Huang, H. Zhang, J. Pei, J. Ou, G. Yuan, Potential biodegradable Zn-Cu binary alloys developed for cardiovascular implant applications, Journal of the Mechanical Behavior of Biomedical Materials, 2017, **72** (8), 182.

[7] Y. Hou, G. Jia, R. Yue, Synthesis of biodegradable Zn-based scaffolds using NaCl templates: Relationship between porosity, compressive properties and degradation behaviour, Materials Characterization, 2018, **137 (**3), 162.

[8] Z. Cui, W. Li, L. Cheng, D. Gong, W. Cheng, W. Wang, Effect of nano-HA content on the mechanical properties, degradation and biocompatible behavior of Mg-Zn/HA composite prepared by spark plasma sintering, Materials Characterization, 2019, **151 (5)**, 620.

[9] Y. Yan, Y. Kang, D. Li, K. Yu, T. Xiao, Q. Wang, Microstructure, Mechanical Properties and Corrosion Behavior of Porous Mg-6 wt.% Zn Scaffolds for Bone Tissue Engineering , Journal of Materials Engineering and Performance, 2018, **27** (3), 970.

[10] S. Cai, T. Lei, N. Li, F. Feng, Effects of Zn on microstructure, mechanical properties and corrosion behavior of Mg–Zn alloys, Materials Science and Engineering: C, 2012, **32** (8), 2570.

[11] S. Zhang, X. Zhang, C. Zhao, J. Li, Y. Song, C. Xie, Research on an Mg-Zn alloy as a degradable biomaterial, Acta Biomaterialia,2010, **6** (2), 626.

[12] C. Prakash, S. Singh, K. Verma, S.S. Sidhu, S. Singh, Synthesis and characterization of Mg-Zn-Mn-HA composite by spark plasma sintering process for orthopedic applications, Vacuum, 2018, **155** (9), 578.

[13] P. Guo, Z. Cui, L. Yang, L. Cheng, W. Wang, B. Xu, Preparation of Mg/Nano-HA Composites by Spark Plasma Sintering Method and Evaluation of Different Milling Time Effects on Their Microhardness, Corrosion Resistance, and Biocompatibitity, Advanced Engineering Materials, 2017, **19** (1), 276.

[14] L. Zhang, Z.Y. He, J. Tan, M. Calin, K.G. Prashanth, B. Sarac, Designing a multifunctional Ti-2Cu-4Ca porous biomaterial with favorable mechanical properties and high bioactivity,Journal of Alloys and Compounds, 2017, **727** (12), 338.

[15] O. Balci, U. Burkhardt, M.S. Schmidt, J. Hennick, M.B. Yağci, M. Somer, Densification, microstructure and properties of TiB2 ceramics fabricated by spark plasma intering, Materials Characterization, 2018, **145** (11), 435.

[16] S. Amukarimi, M. Mozafari, Biodegradable magnesium-based biomaterials: An overview of challenges and opportunities, MedComm., 2021, 2, 123.

[17] S. Prasadh, V. Ratheesh, V. Manakari, G. Parande, M. Gupta, R. Wong, The Potential of Magnesium Based Materials in Mandibular Reconstruction, Metals, 2019, **9** (3), 302.

[18] Haghshenas M., Mechanical characteristics of biodegradable magnesium matrix composites: A Review, Journal of Magnesium and Alloys, 2017, **5** (2), 189.

[19] I. Nakahata, Y. Tsutsumi, E. Kobayashi, Mechanical Properties and Corrosion Resistance of Magnesium–Hydroxyapatite Composites Fabricated by Spark Plasma Sintering, Metals, 2020, **10** (10), 1314.

[20] I. N. Popescu, R. Vidu, V. Bratu, Porous Metallic Biomaterials Processing (Review) Part 1: Compaction, Sintering Behavior, Properties and Medical Applications Scientific Bulletin of "Valahia" University Materials and Mechanics., 2017, **15** (13),28.

[21] I. Antoniac, M. D. Vrânceanu, A. Antoniac, The influence of the magnesium powder used as reinforcement material on the properties of some collagen based composite, Journal of Optoelectronics and advanced Materials, 2013, **15** (7-8), 667.

[22] A.I. Bita, A. Antoniac, C. Cotrut, E. Vasile, I. Ciuca, M. Niculescu, I. Antoniac, In vitro Degradation and Corrosion Evaluation of Mg-Ca Alloys for Biomedical , Journal of Optoelectronics and advanced Materials, 2016, **18** (3-4), 394.

[23] D. Merson, A. Brilevsky, P. Myagkikh, A. Tarkova, A. Prokhorikhin, E. Kretov, T. Frolova, A. Vinogradov, The Functional Properties of Mg–Zn–X Biodegradable Magnesium Alloys, Materials, 2020, **13** (3), 544.

[24] S. Erdibil, S. Cesur, R. İpek, Mg/Zn composites produced by mechanical alloying and hot pressing and in-vitro biodegradation, J. Eng. Sci., Usak University Journal of Engineering Sciences, 2019, **2** (1), 22.

[25] MP. Staiger, AM. Pietak, J. Huadmai, G. Dias, Magnesium and its alloys as orthopedic biomaterials: A Review, Biomaterials, 2006, **27** (9), 1728.

[26] T. Kokubo, H.Takadama, How useful is SBF in predicting in vivo bone bioactivity? Biomaterials, **27** (15), 2907 (2006).

[27] Kessel, H.U.; Hennicke, J.; Schmidt, J.; Weißgärber, T.; Kieback, B.F.; Herrmann, M.; Räthel, J. "FAST" field assisted sintering technology - A new process for the production of metallic and ceramic sintering materials. In Pulvermetallurgie in Wissenschaft und Praxis 22 - Pulvermetallurgie -Kompetenz und Perspektive; Heimdall Verlag: Witten, Germay, 2006, 201-238.

[28] M. Cojocaru,Producerea și procesarea pulberilor metalice, Editura Matrix Rom, București, 1997.

****